# Supplementary information

**Supplementary table 1. *YAP* gene alterations in gynecological cancers.**

| Cancer types | Total cases | Total Alterations | Amplifications | Deletions | Mutations |
|---|---|---|---|---|---|
| Cervical | 36 | 6 (16.7%) | 6 (16.7%) | 0 | 0 |
| Ovarian | 316 | 26 (8.2%) | 23 (7.3%) | 2 (0.6%) | 1 (0.3%) |
| Ov. HGSC | 279 | 24 (8.6%) | 22 (7.9%) | 2 (0.7%) | 0 |
| Uterine[27] | 240 | 10 (4.2%) | 2 (0.8%) | 4 (1.7%) | 4 (1.7%) |
| Breast[26] | 482 | 6 (1.2%) | 4 (0.8%) | 1 (0.2%) | 1 (0.2%) |

Note: Ov.HGSC: Ovarian high-grade serous carcinoma

Supplementary information

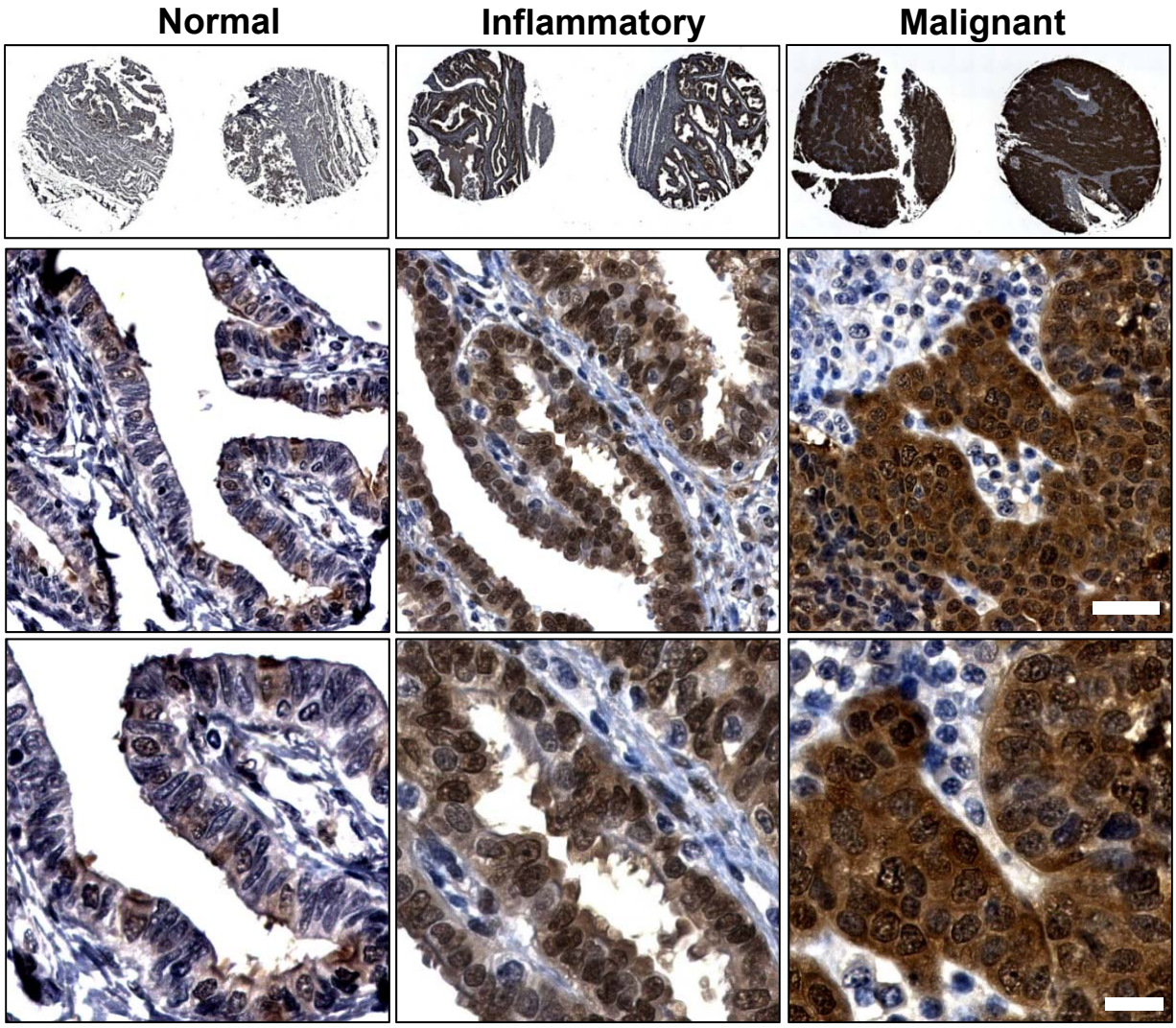


**Supplementary figure 1. Expression of YAP in human fallopian tube tissues**. Expression of YAP protein in normal, inflammatory and cancerous fallopian tube tissues is determined by immunohistochemistry. YAP protein immunosignal is shown as brown. Cell nuclei are counter-stained with hematoxylin (blue). a) Top panel: representative images showing YAP staining pattern in normal, chronic inflammation and cancerous tissues in a tissue microarray; Middle panel: representative images showing the immunosignal distribution and intensity in normal, inflammatory and cancerous fallopian tube tissues; Scale bar: 50 μm. Lower panel: representative high-resolution images showing the cellular distribution YAP immunosignal in normal, inflammatory and cancerous fallopian tube tissues. Scale bar: 20μm.

# Supplementary information

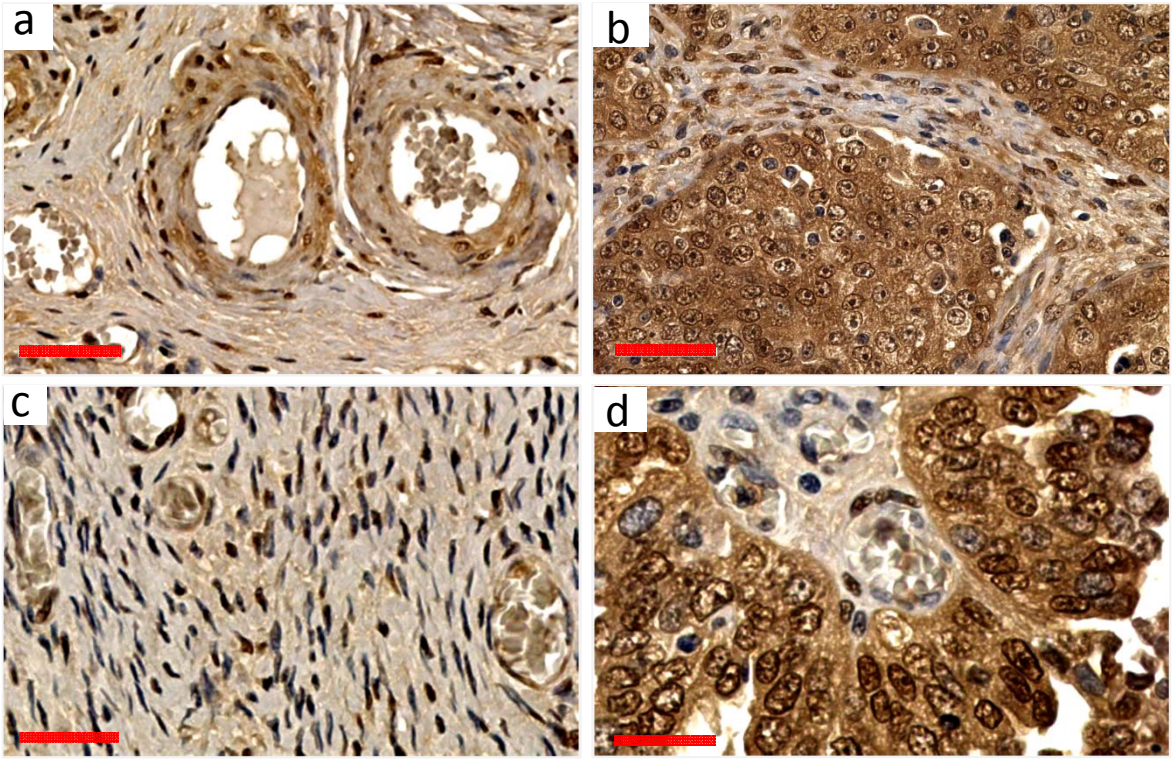


**Supplementary figure 2. Overexpression of YAP in human ovarian high grade serous carcinoma (HGSC)**. Expression of YAP protein in age-matched normal ovarian tissues and ovarian HGSC is determined by immunohistochemistry. YAP protein immunosignal is shown as brown. Cell nuclei are counter-stained with hematoxylin (blue). a & b) Representative images showing YAP immunosignal distribution and intensity in normal ovarian tissues (a) and ovarian HGSC (b). Scale bar: 50 μm. c & d) Representative high-resolution images showing the cellular distribution of YAP immunosignal in normal ovarian tissues (c) and ovarian HGSC (d). Scale bar: 25 μm.

Supplementary information

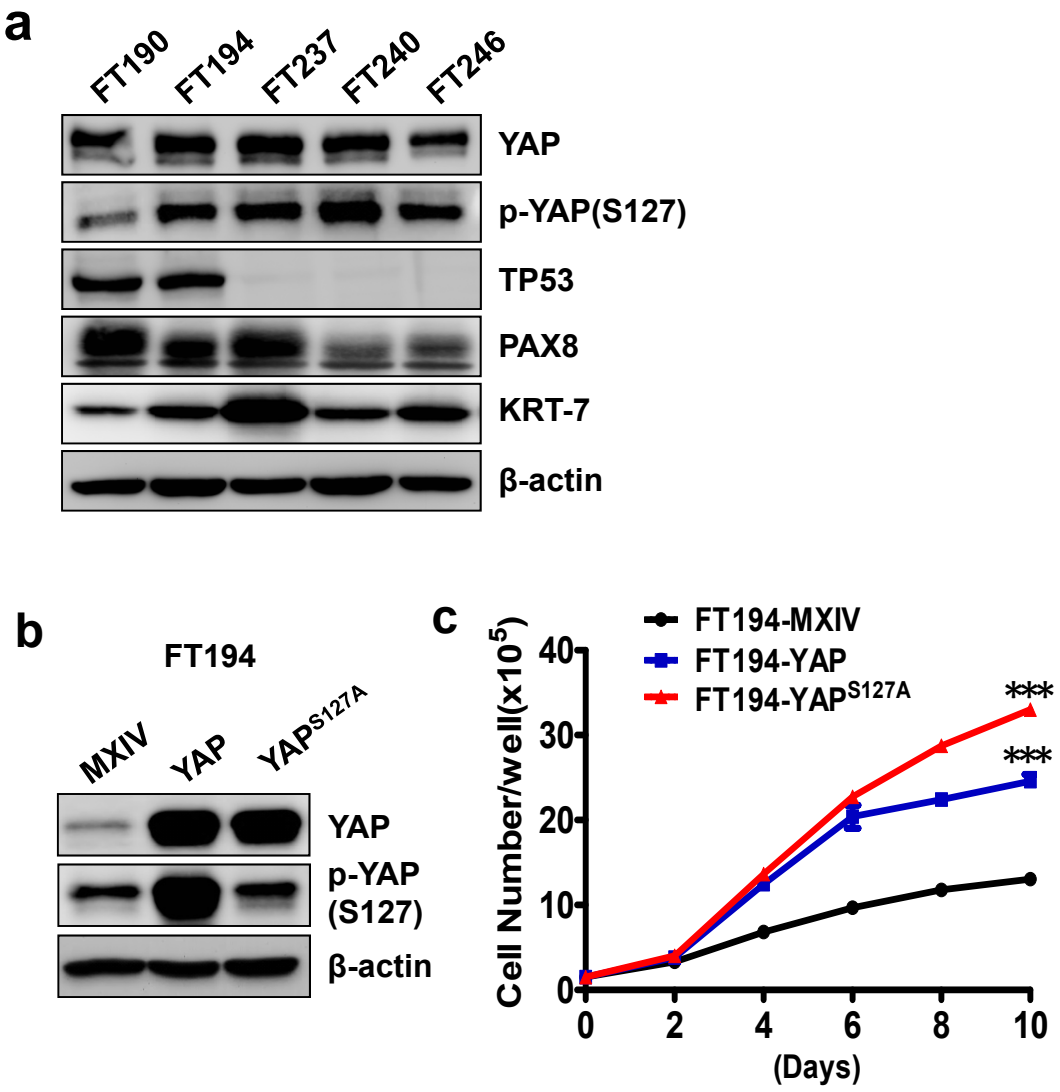


**Supplementary figure 3. YAP protein levels in FTSEC cell lines. a**) Expression of YAP, phosphorylated YAP [p-YAP (S127)], TP53, PAX8 and cytokeratin 7 (KRT-7) proteins in five FTSEC cell lines. β-actin was used as a loading control. **b**) Expression of YAP and phosphorylated YAP (S127) in FT194-MXIV, FT194-YAP and FT194-YAP$^{S127A}$ cell lines determined by Western blot. β-actin was used as a loading control. **c**) Growth curves of FT194-MXIV, FT194-YAP and FT194-YAP$^{S127A}$ cell lines. Each point on the growth curves represents the mean ± SEM (n=4). ***: $P < 0.001$ compared with FT194-MXIV control on day 10.

Supplementary information

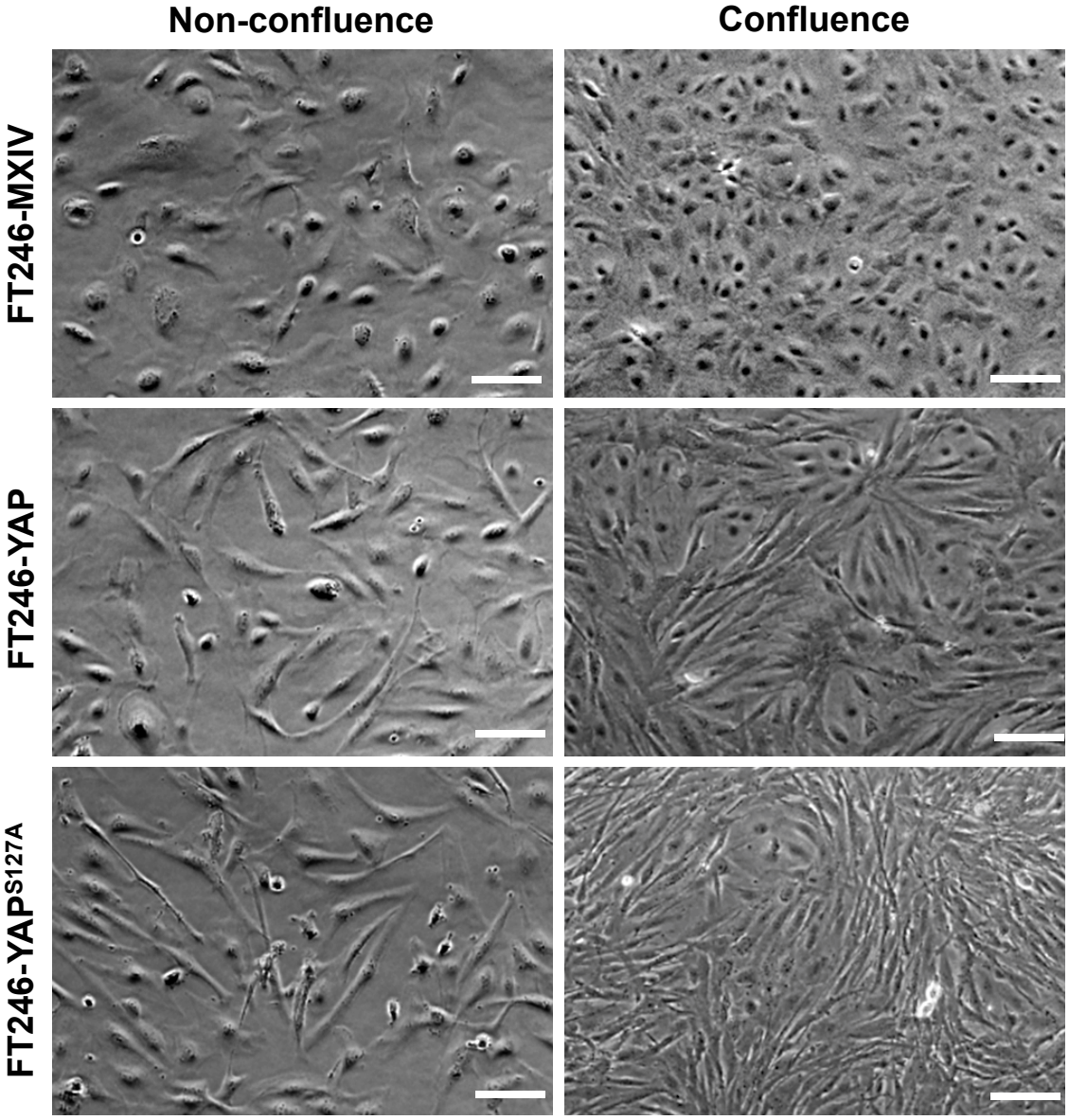


**Supplementary figure 4. YAP treatment results in morphological change of FTSECs.** Left column: morphology of FT246-MXIV, FT246-YAP and FT246-YAP$^{S127A}$ cells before cells reach 100% confluence. Right column: morphology of FT246-MXIV, FT246-YAP and FT246-YAP$^{S127A}$ cells after cells reach confluence. Scale bar: 100 μm.

Supplementary information

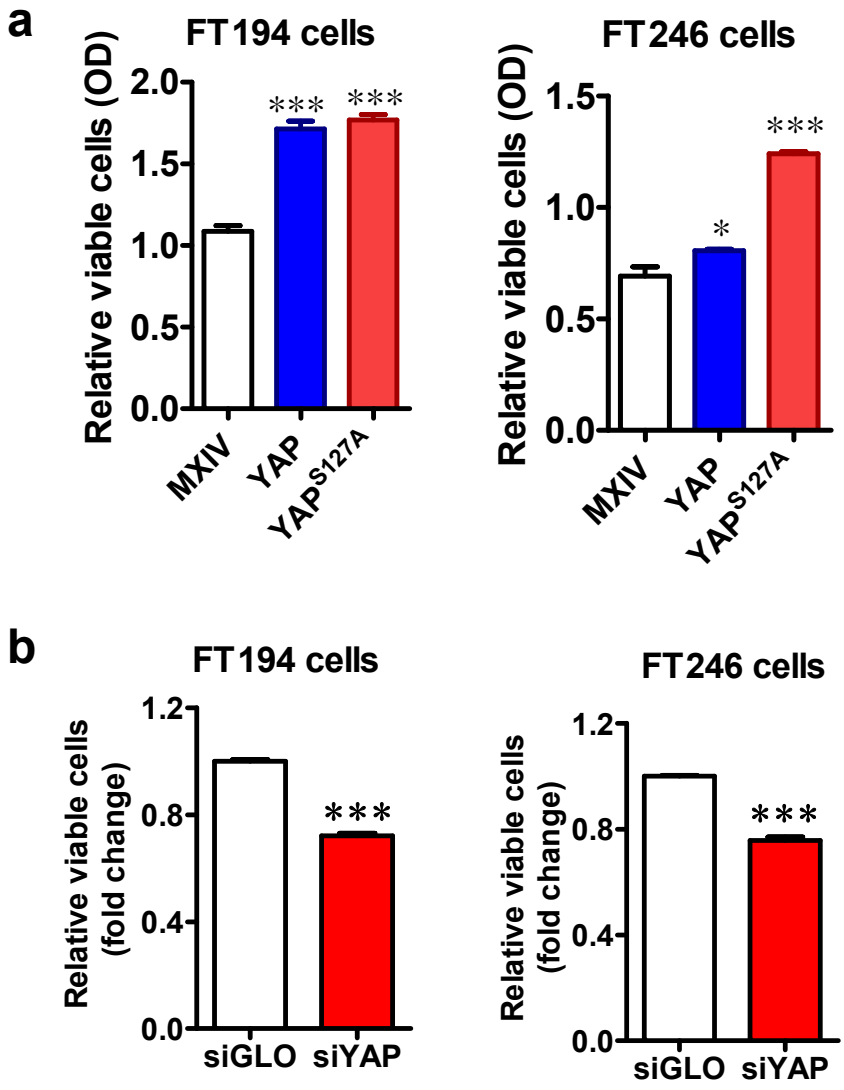


**Supplementary Figure 5. YAP regulates cell proliferation/viability in FTSECs**. **a**) MTT assay showing relative viable cells in FT194-MXIV, FT194-YAP and FT194-YAP$^{S127A}$ cells and FT246-MXIV, FT246-YAP and FT246-YAP$^{S127A}$ cells. Each bar represents the mean ± SEM of at least three independent assays. *: $P < 0.05$ compared with empty vector (MXIV) transfected control cells. ***: $P < 0.001$ compared with MXIV control cells. **b**) MTT assay showing relative viable cell numbers in FT194 and FT246 cells with or without knockdown of YAP using YAP siRNA (siYAP). Each bar represents the mean ± SEM of at least three independent assays. ***: $P < 0.001$ compared with the non-targeting siRNA transfected control cells (siGLO).

Supplementary information

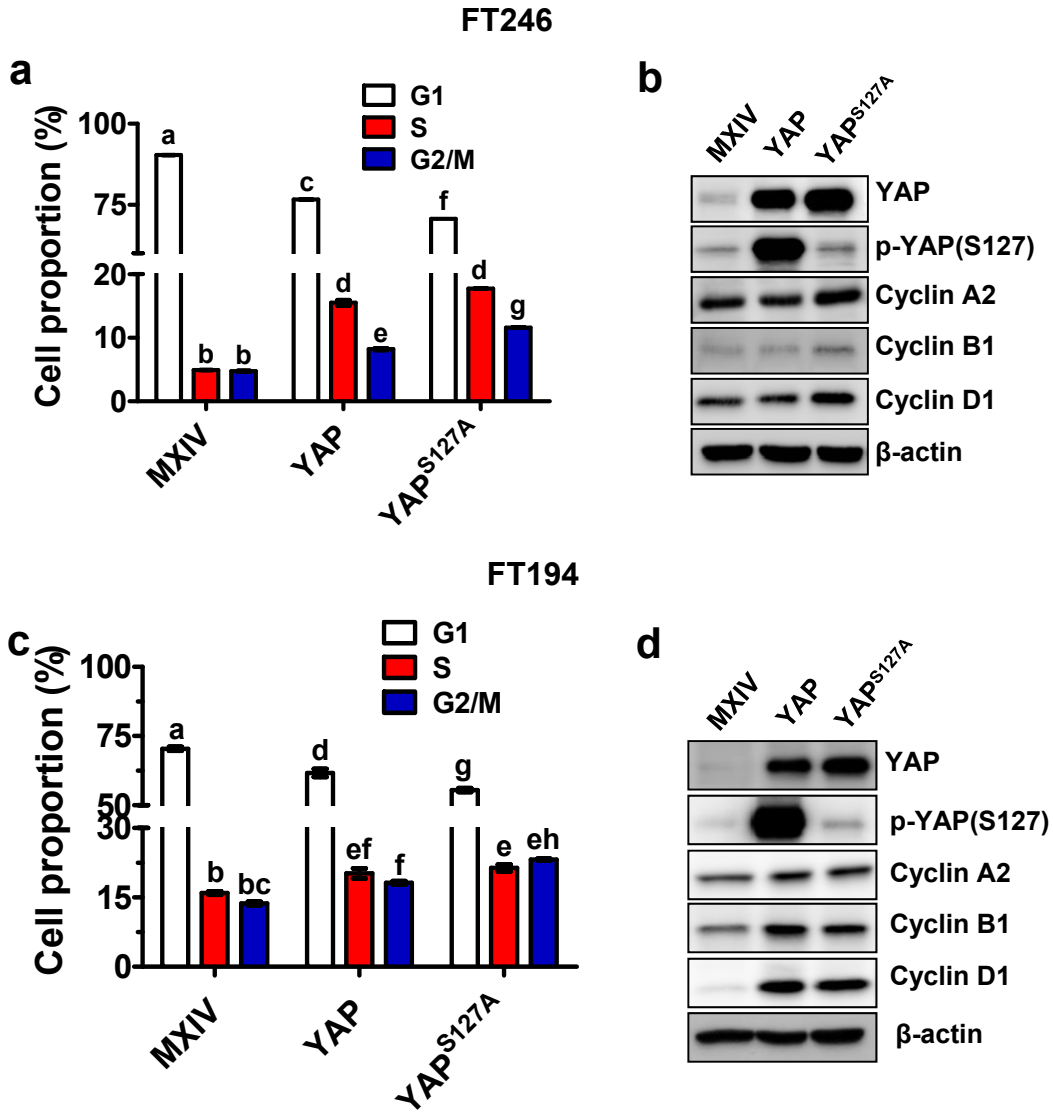


**Supplementary figure 6. YAP promotes cell cycle progression in FTSECs**. a) Flow cytometry analysis showing cell cycle distribution in FT246-MXIV, FT246-YAP and FT246-YAP$^{S127A}$ cells. Each bar represents the mean ± SEM of three independent assays. b) Immunoblot results showing protein levels of total YAP, phosphorylated YAP[p-YAP(S127)] and Cyclins associated with cell cycle progression in FT246-MXIV, FT246-YAP and FT246-YAP$^{S127A}$ cells. c) Flow cytometry analysis showing cell cycle distribution in FT194-MXIV, FT194-YAP and FT194-YAP$^{S127A}$ cells. Each bar represents the mean ± SEM of three independent assays. d) Immunoblot results showing protein levels of total YAP, phosphorylated YAP[p-YAP(S127)] and Cyclins associated with cell cycle progression in FT194-derived cell lines. Bars with the same letters are not significantly different from each other ($P < 0.05$).

Supplementary information

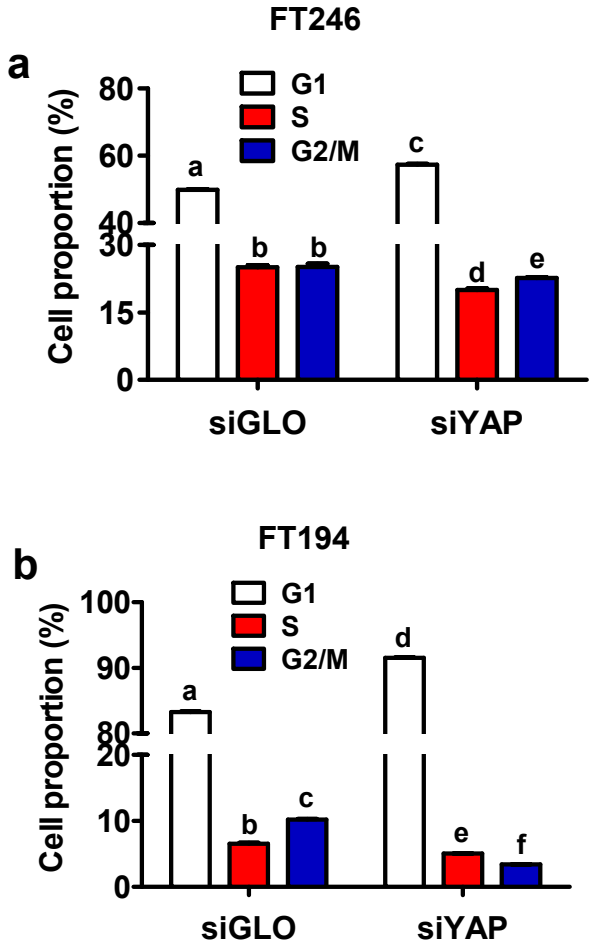


**Supplementary figure 7. Knockdown of YAP suppresses cell cycle progression in FTSECs.** a) Flow cytometry data showing cell cycle distributions in FT246 cells with or without knockdown of YAP protein using YAP siRNA (siYAP). A fluorescein-labeled non-targeting siRNA (siGLO) was used as a negative control. Each bar represents the mean ± SEM of three independent experiments. b) Flow cytometry analysis showing cell cycle distributions in FT194 cells with (siYAP) or without (siGLO) knockdown of YAP protein with YAP siRNA. Each bar represents the mean ± SEM of three independent experiments. Bars with different letters are significantly different from each other ($P < 0.05$).

Supplementary information

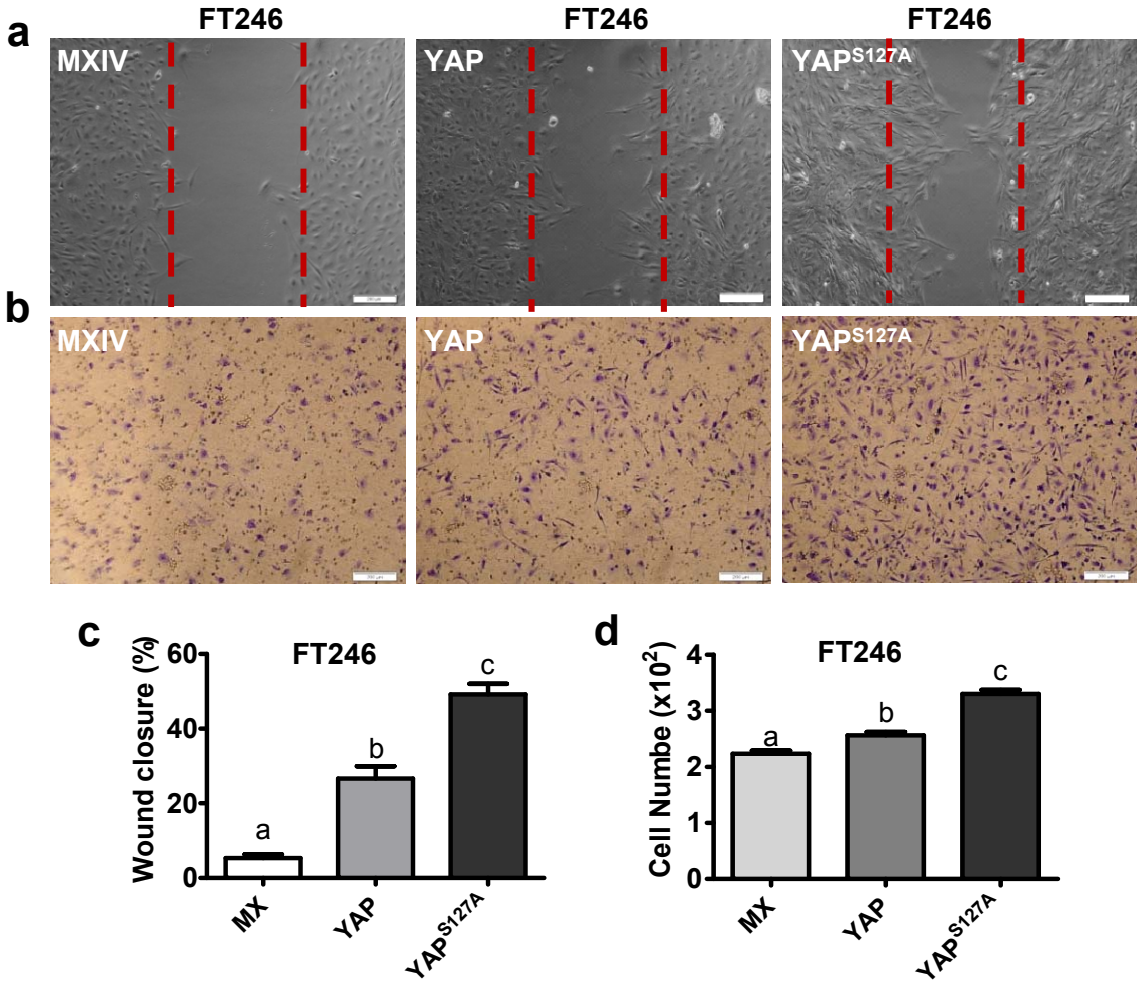


**Supplementary figure 8. YAP stimulates migration of FT246 cells. a**) Representative images showing the motility of FT246-MXIV (control), FT246-YAP and FT246-YAP$^{S127A}$ cells as determined by a wound healing assay. Scale bar: 200μm. **b**) Representative images showing the motility of FT246-MXIV (control), FT246-YAP and FT246-YAP$^{S127A}$ cells as determined by a Transwell assay. Scale bar: 200μm. **c**) Quantitative data showing percentages of wound closure in three FT246 cell lines in a). **d**) Quantitative data showing the number of cells migrated through the chamber membrane in the Transwell assay in three FT246 cell lines in b). Scale bar: 200μm. Each bar represents the mean ± SEM of at least three independent experiments. Bars with different letters are significantly different from each other ($P < 0.05$).

Supplementary information

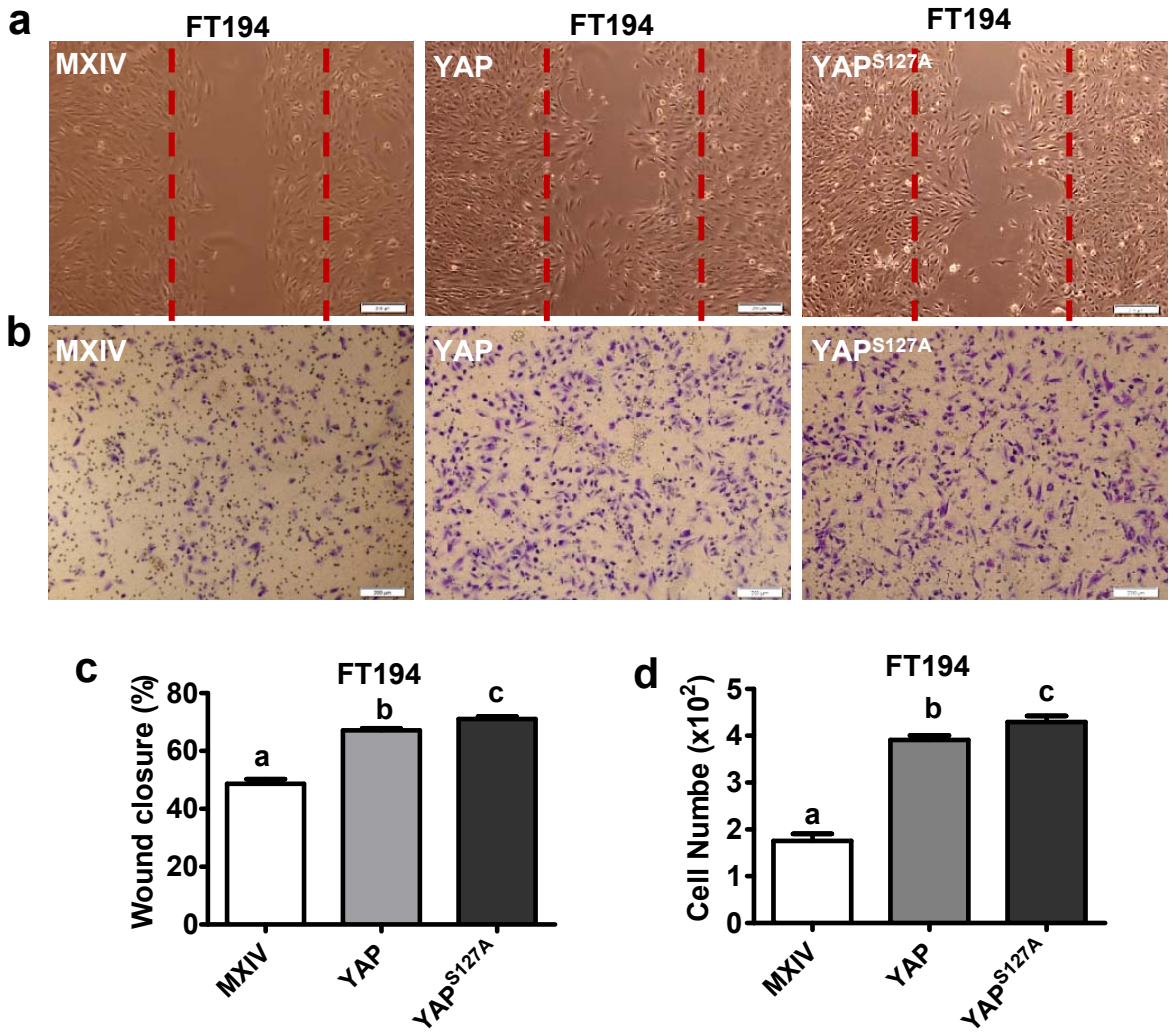


**Supplementary figure 9. YAP stimulates migration of FT194 cells.** a) Representative images showing the motility of FT194-MXIV (control), FT194-YAP and FT194-YAP$^{S127A}$ cells as determined by a wound healing assay. **b**) Representative images showing the motility of FT194-MXIV (control), FT194-YAP and FT194-YAP$^{S127A}$ cells as determined by Transwell assay. **c**) Quantitative data showing percentages of wound closure in three F194 cell lines in a). **d**) Quantitative data showing the number of cells migrated through the chamber membrane in the Transwell assay in three FT194 cell lines in b). Each bar represents mean ± SEM of at least three independent experiments. Bars with different letters are significantly different from each other ($P < 0.01$). Scale bar: 200μm.

Supplementary information

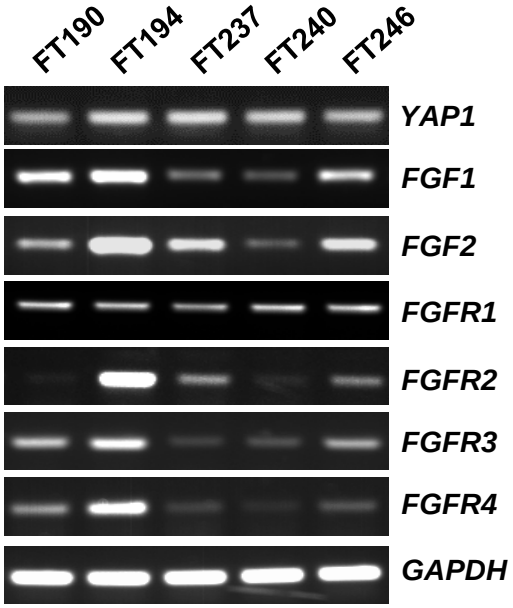


**Supplementary figure 10. Expression of *YAP1* and *FGFs/FGFRs* in the FTSECs.** RT-PCR was used to determine mRNA expression of *YAP1, FGF1/2, and FGFRs* in five fallopian tube secretory epithelial cell lines. *GAPDH* was used as a mRNA loading control. Experiment has been repeated at least three times and the representative images were presented.

Supplementary information

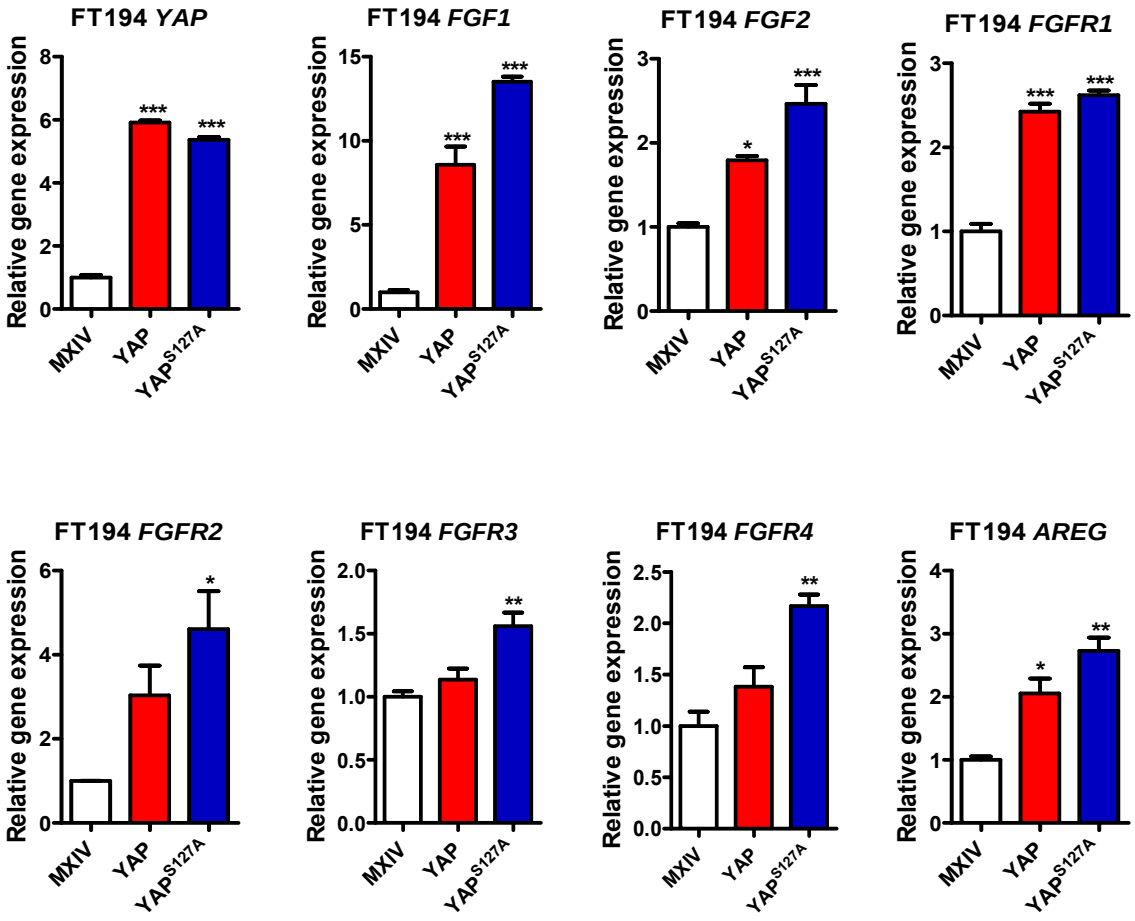


**Supplementary figure 11. Effect of YAP on the expression of *FGF* ligands and receptors in FT194 cells.** mRNA levels of *YAP, FGF1/2, FGFRs* in FT194-MXIV (control), FT194-YAP, and FT194-YAP$^{S127A}$ cells were determined using RT-PCR. mRNA signal intensity was quantified using NIH imageJ software and normalized to *GAPDH*. Relative mRNA expression levels were presented as ratio (relative to mRNA level of FT194-MXIV in each group). Each bar represents the mean ± SEM of three independent experiments. * : $P < 0.05$ compared to MXIV control; ** : $P < 0.01$ compared to MXIV control; *** : $P < 0.001$ compared to MXIV control. Quantification data showing that overexpression of wild type YAP or constitutively active YAP significantly increase mRNA expression of basic and acidic *FGF*s and *FGFR*s in FT194 cells.

# Supplementary information

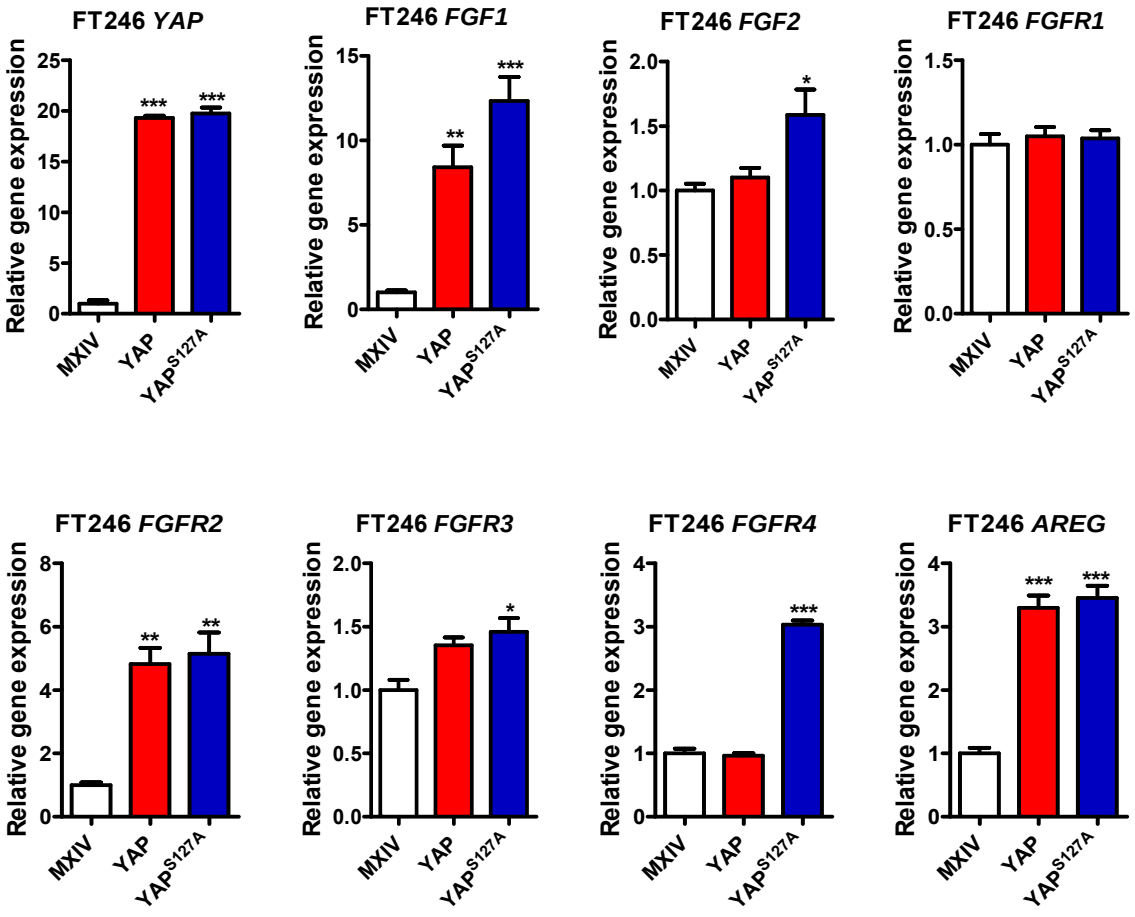


**Supplementary figure 12. Effect of YAP on the expression of *FGF* ligands and receptors in FT246 cells.** mRNA levels of *YAP, FGF1/2, FGFRs* in FT246-MXIV (control), FT246-YAP, and FT246-YAP$^{S127A}$ cells were determined using RT-PCR. mRNA signal intensity was quantified using NIH imageJ software and normalized to *GAPDH*. Relative mRNA expression levels were presented as ratio (relative to mRNA level of FT246-MXIV in each group). Each bar represents the mean ± SEM of three independent experiments. * : $P < 0.05$ compared to MXIV control; ** : $P < 0.01$ compared to MXIV control; *** : $P < 0.001$ compared to MXIV control. Quantification data showing that overexpression of wild type YAP or constitutively active YAP significantly increase mRNA expression of basic and acidic *FGF*s and *FGFR*s in FT246 cells.

Supplementary information

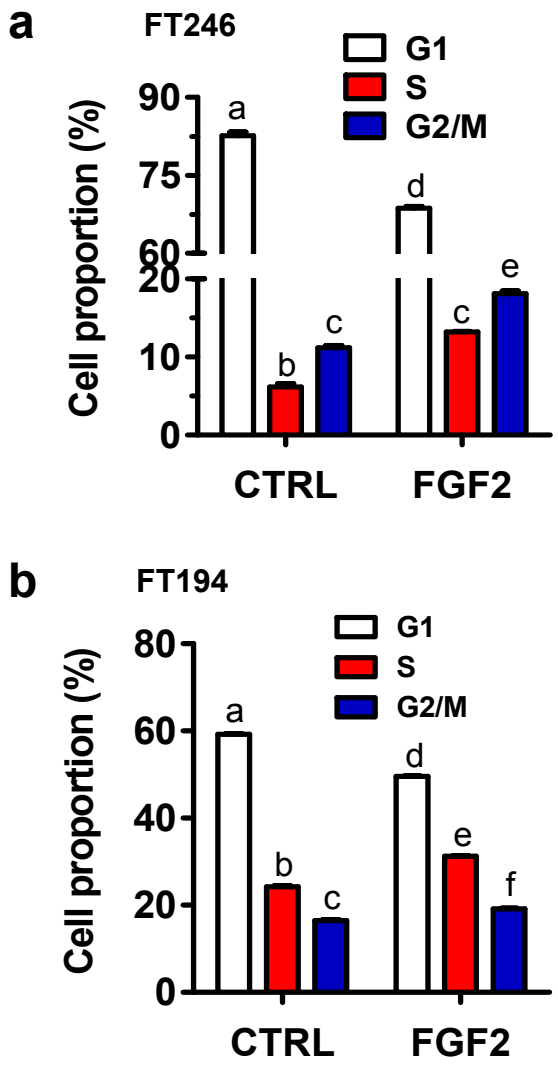


**Supplementary figure 13. FGF2 promotes cell cycle progression in FTSECs**. a) Treatment of FT246 cells with basic FGF (20ng/ml) significantly increased portions of cells in S and G2/M phases and decreased the portion of cells in G1 phase. b) Treatment of FT194 cells with basic FGF (20ng/ml) significantly increased portions of cells in S and G2/M phases and decreased the portion of cells in G1 phase. CTRL: control; FGF2: basic FGF, 20ng/ml. Each bar represents the mean ± SEM of three independent experiments. Bars with different letters are significantly different from each other ($P < 0.05$).

Supplementary information

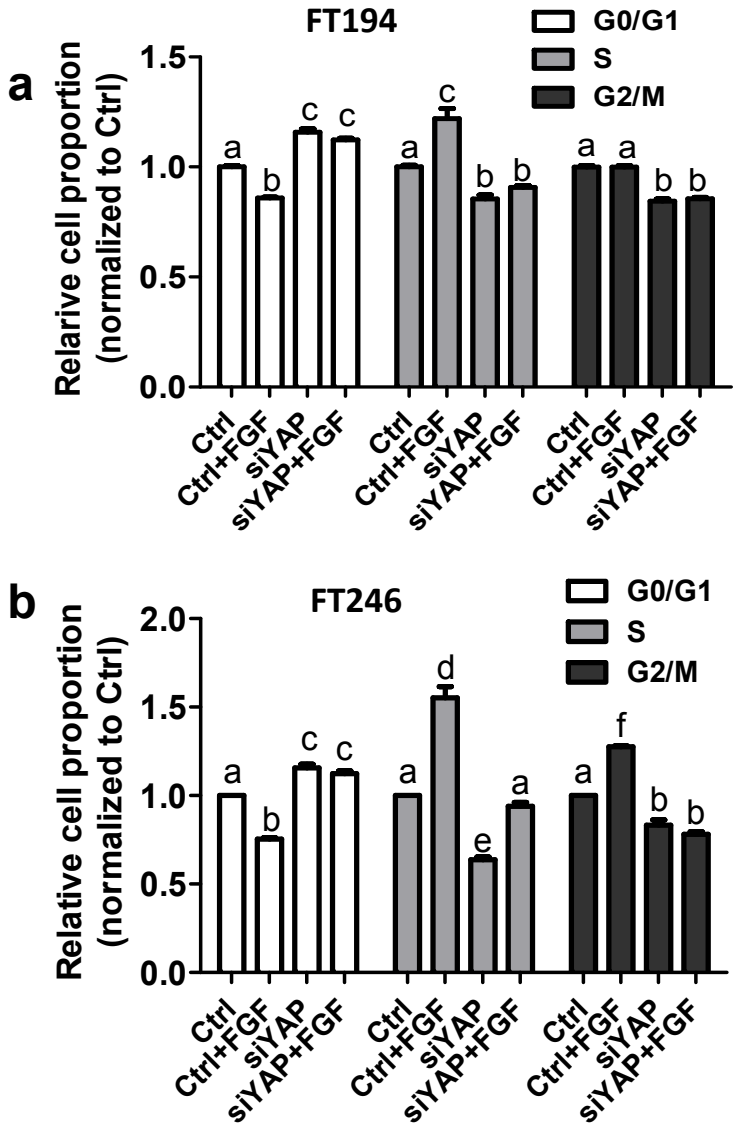


**Supplementary figure 14. YAP is required for FGF promotion of cell cycle progression in FTSECs.** a) Knockdown of YAP with YAP siRNA (siYAP) significantly blocked FGF2-induced increase in portions of cell in S phase and decrease in the portion of cells in G0/G1 phase in FT194 cells. b) Knockdown of YAP with YAP siRNA (siYAP) blocked FGF2-induced increase in portions of cells in S and G2/M phase and FGF2-induced decrease in the portion of cells in G0/G1 phase in FT246 cells. Ctrl: non-targeting siRNA transfected cells used as control; FGF: basic FGF (20ng/ml, 24h); siYAP: YAP siRNA. Each bar represents the mean ± SEM of three independent experiments. Bars with different letters are significantly different from each other ($P < 0.05$).

Supplementary information

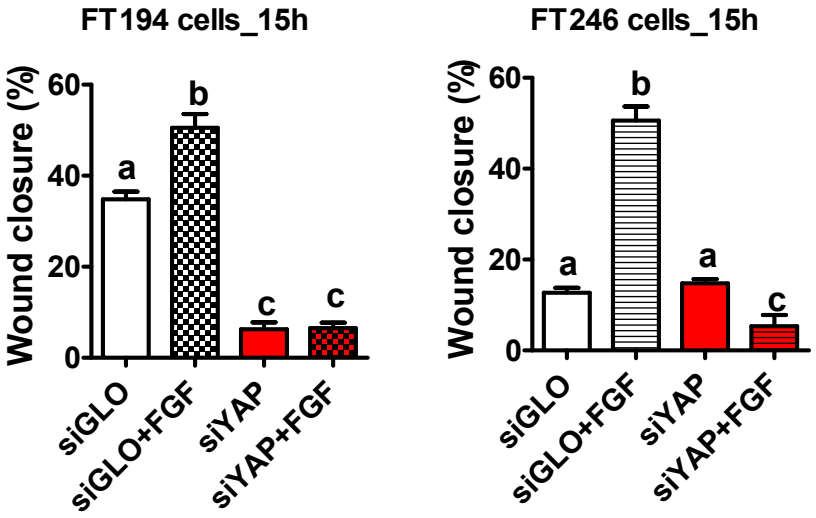


**Supplementary figure 15. YAP is required for FGF regulating migration of FTSECs.** Quantitative results of figure 8b showing the percentage of wound closure in the wound healing assays in FT194 and FT246 cells. Each bar represents the mean ± SEM of three independent experiments. Bars with different letters are significantly different from each other ($P$<0.001).

Supplementary information

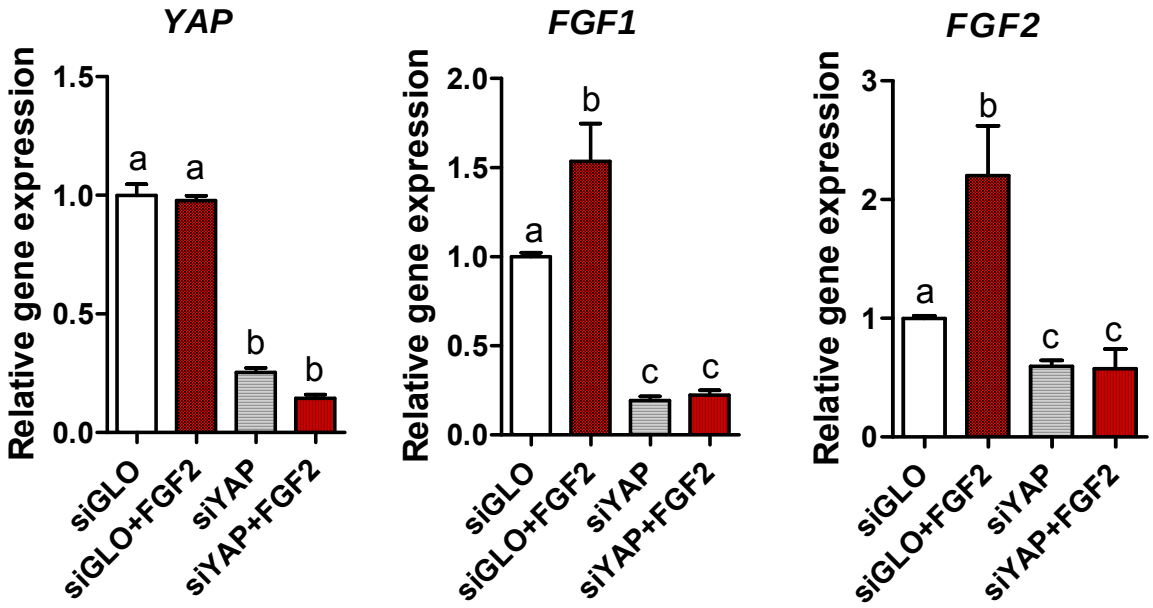


**Supplementary figure 16. YAP is required for FGF autocrine/paracrine regulation**. FT246 cells were transfected with non-targeting siRNA (siGLO) or YAP siRNA (siYAP) before treatment with or without FGF2 (10ng / ml) for 48h. *YAP*, *FGF1* and *FGF2* mRNA was detected with RT-PCR. mRNA signal intensity was quantified using NIH ImageJ and normalized to *GAPDH*. Data are presented as ratio of siGLO control in each group. Bars represents the mean ± SEM of three repeats. Bars with different letters are significantly different from each other ($P < 0.05$).

Supplementary information

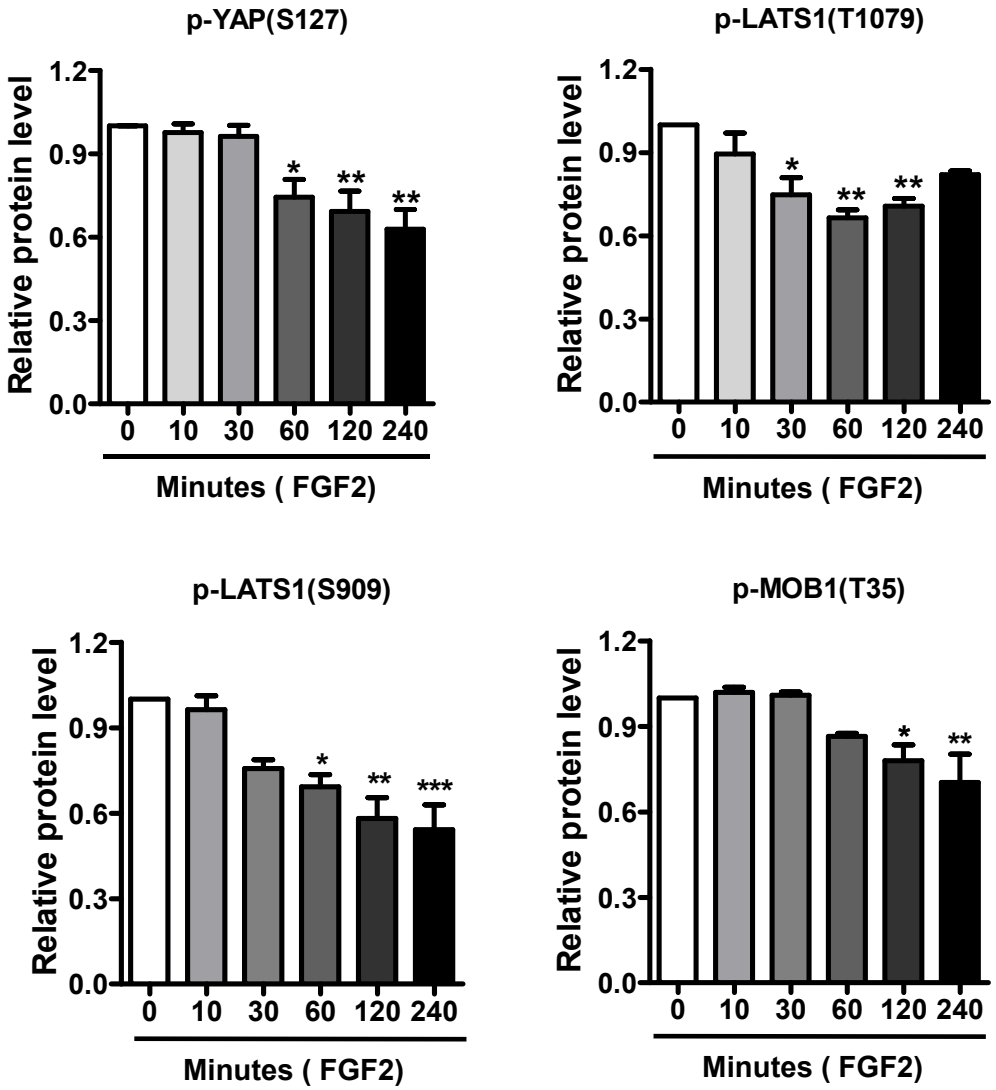


**Supplementary figure 17. Involvement of the Hippo pathway in FGF regulation of FTSECs.** Quantitative results of Figure 9a showing that treatment of FT194 cells with FGF2 (20 ng/ml) rapidly and significantly suppressed phosphorylation of the major components of the Hippo/YAP signaling pathway (LATS1, Mob1 and YAP). Signal intensity in each group were normalized to the control (vehicle treatment, indicated as 0 minute FGF2 treatment in graphs) and were presented as a ratio. Each bar represents the mean ± SEM of at least three experiments. * : $P < 0.05$; **: $P < 0.01$; *** : $P < 0.001$.

Supplementary information

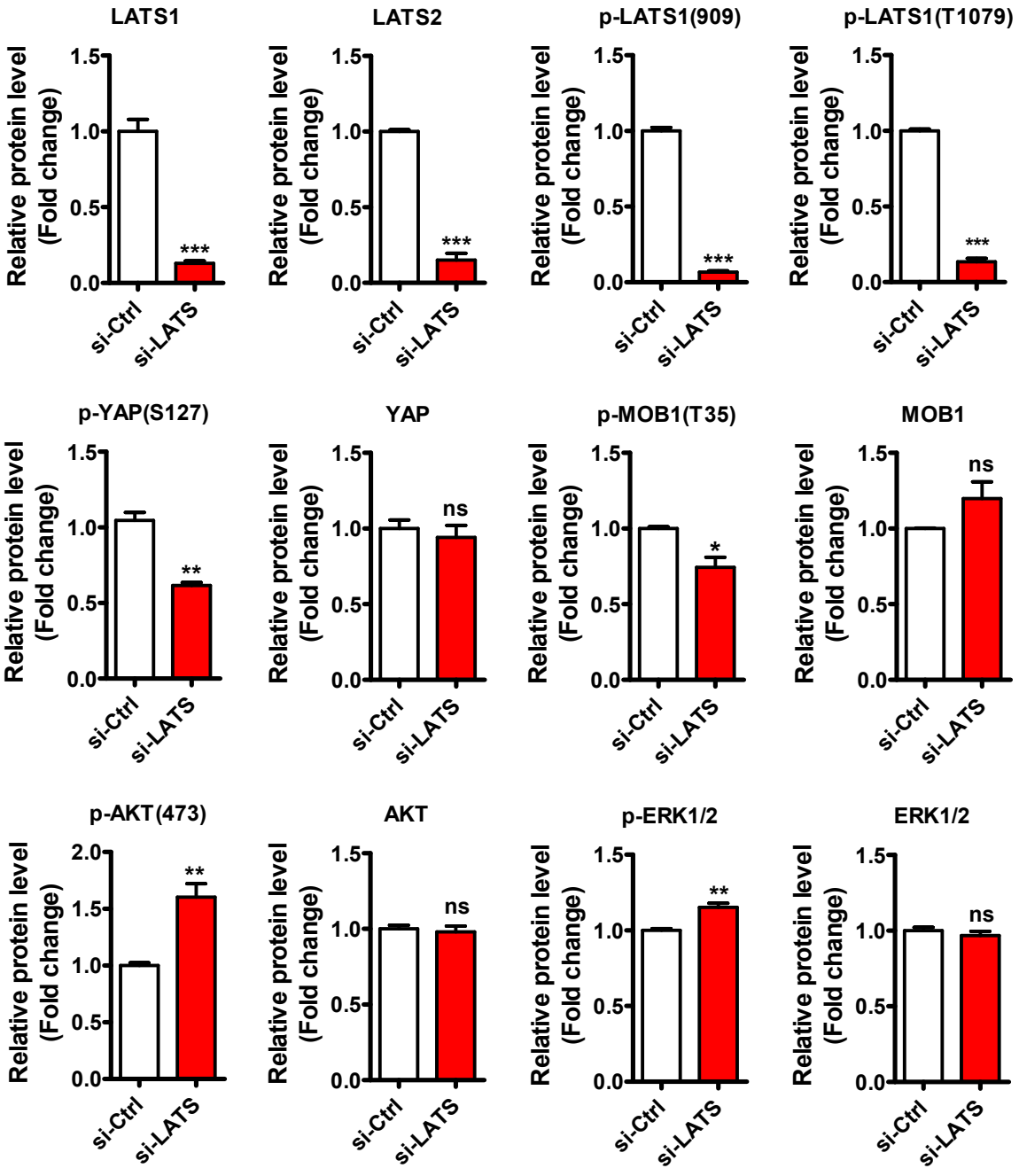


**Supplementary figure 18. Effect of LATS1/2 on the expression and activation of major components of several signaling pathways in FTSECs.** LATS1/2 double knockdown suppressed the Hippo pathway, activated YAP, AKT, and ERK1/2 in FTSECs. Total and phosphorylated proteins levels were determined using Western blot and quantified using NIH imageJ software. Relative protein levels are presented as ratio (relative to protein level of control (si-Ctrl) in each group). Each bar represents the mean ± SEM of three independent experiments. * : $P < 0.05$ compared to control; ** : $P < 0.01$; ***: $P < 0.001$.

Supplementary information

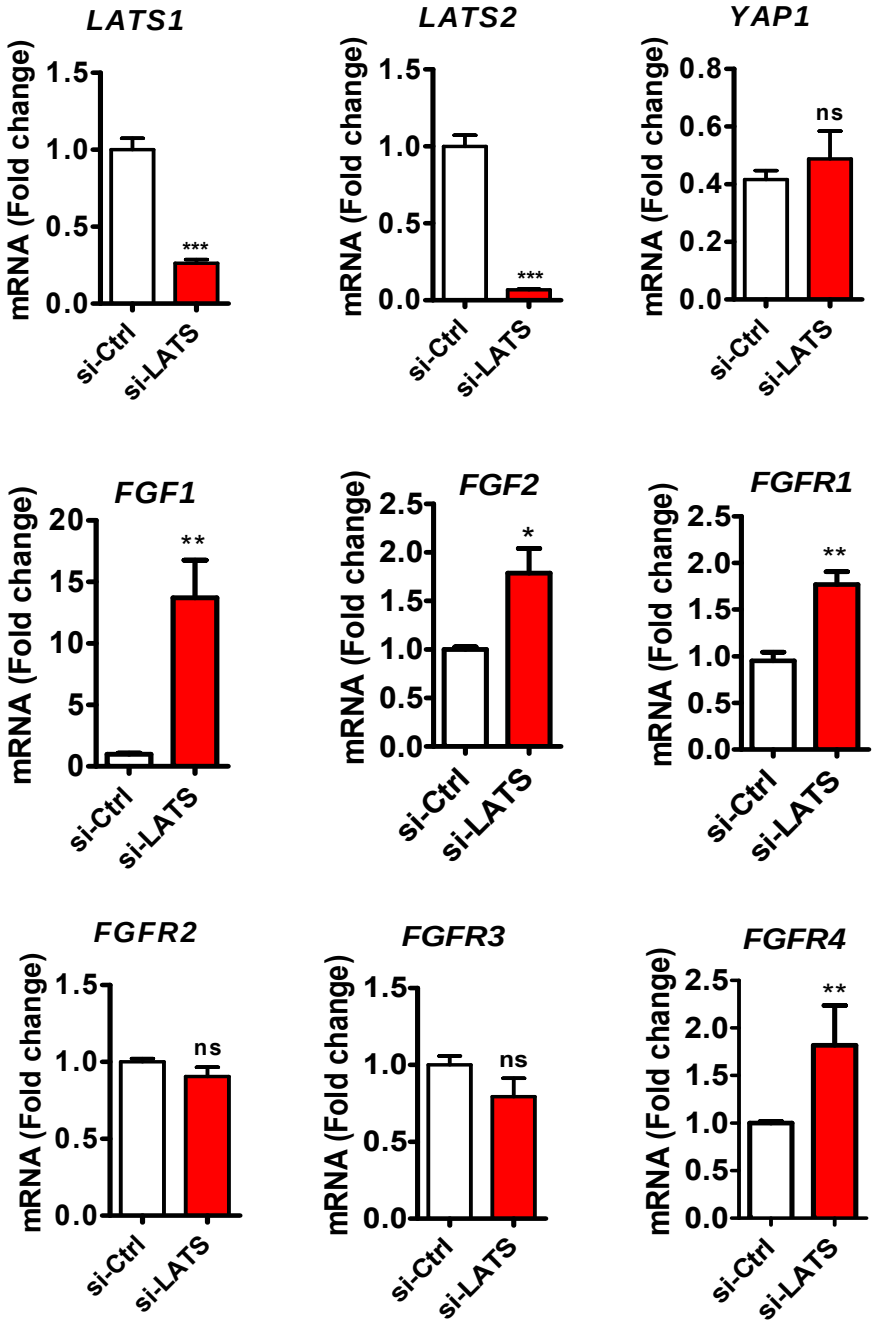


**Supplementary figure 19. Effect of LATS1/2 knockdown on the expression of *FGF* ligands and receptors in FTSECs.** mRNA levels *of LATS1/2*, *YAP1*, *FGF1/2*, *FGFRs* in FT194 cells transfected with non-targeting control siRNA (si-Ctrl) or LATS1/2 siRNAs (si-LATS) were determined using RT-PCR. mRNA signal intensity was quantified using NIH imageJ software and normalized to GAPDH. Relative mRNA expression levels were presented as ratio (relative to mRNA level of si-Ctrl in each group). Each bar represents the mean ± SEM of three independent experiments. * : $P < 0.05$ compared to si-Ctrl; ** : $P < 0.01$ compared to si-Ctrl. ns: No significant difference compared to si-Ctrl.

Supplementary information

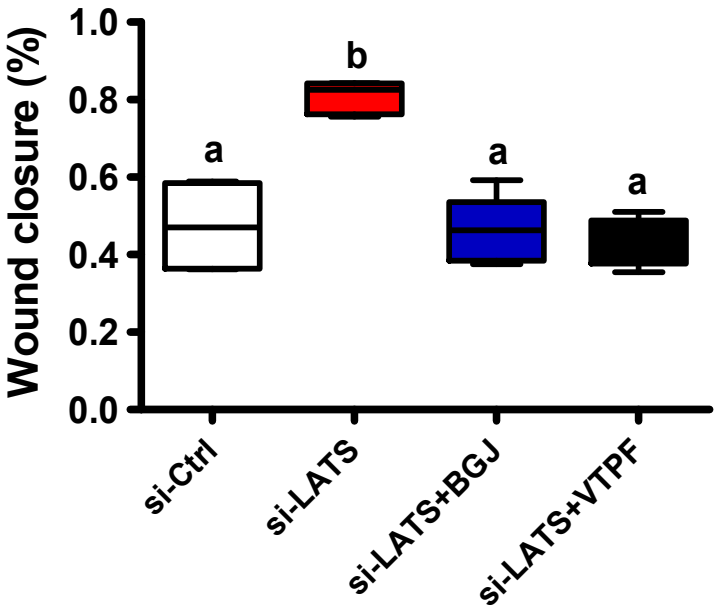


**Supplementary figure 20. Pharmacological inhibition of FGFRs and YAP activity blocks LATS-knockdown-induced cell migration in FTSECs**. FT194 cells were transfected with non-targeting control siRNA (si-Ctrl) or LATS1/2 siRNAs for 6 hrs., Fourty-eight hours after transfection, cells were treated with or without FGFR antagonist BGJ398 (BGJ) and YAP antagonist verteporfin (VTPF) for 15h in a serum-free culture system. Quantitative data showing that treatment of FT194 cells with VTPF or BGJ abolished LATS-knockdown-induced wound closure, which is a indicator of cell migration. Each box represents the mean ± SEM of four to seven independent experiments. Bars with different letters are significantly different from each other ($P < 0.001$).

Supplementary information

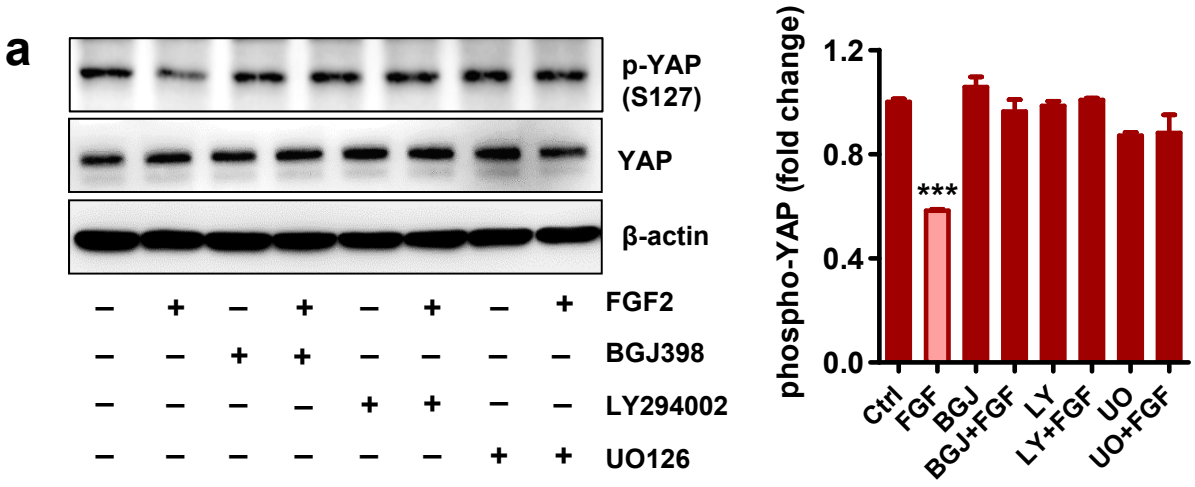


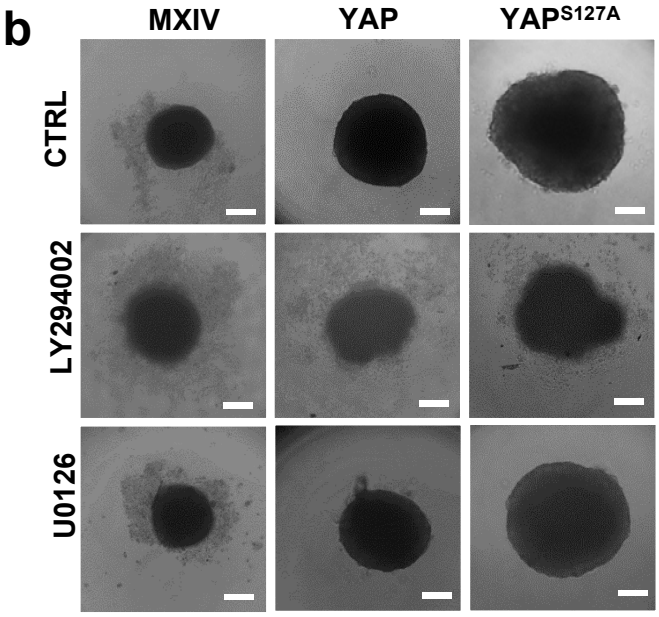


**Supplementary figure 21. Involvement of PI3K and MAPK pathways in FGF2 regulation of YAP activities in FTSECs.** **a**) Left panel: representative blots showing the effect of BGJ398 (FGFR inhibitor, 1μM), LY294002 (PI3K inhibitor, 50μM) and UO126 (MEK kinase inhibitor, 10μM) on FGF2-induced dephosphorylation of YAP (Ser127) in FT194 cells. Right panel: quantitative data showing the fold change of phosphorylated YAP (Ser127) in response to inhibitor treatments. Bars represent the mean ± SEM of three independent experiments. ***: $P < 0.001$ compared to control (Ctrl). **b**) Representative images showing effects of LY294002 and UO126 on FGF2-induced growth of FT194 cells in a 3D-hanging drop culture system. LY294002 drastically blocked YAP-induced growth of FT194 cells in a 3D hanging-drop culture system. UO126 only partially inhibited YAP-induced growth of FT194 cells in the 3D culture. Each experiment was repeated at least three times.

Supplementary information

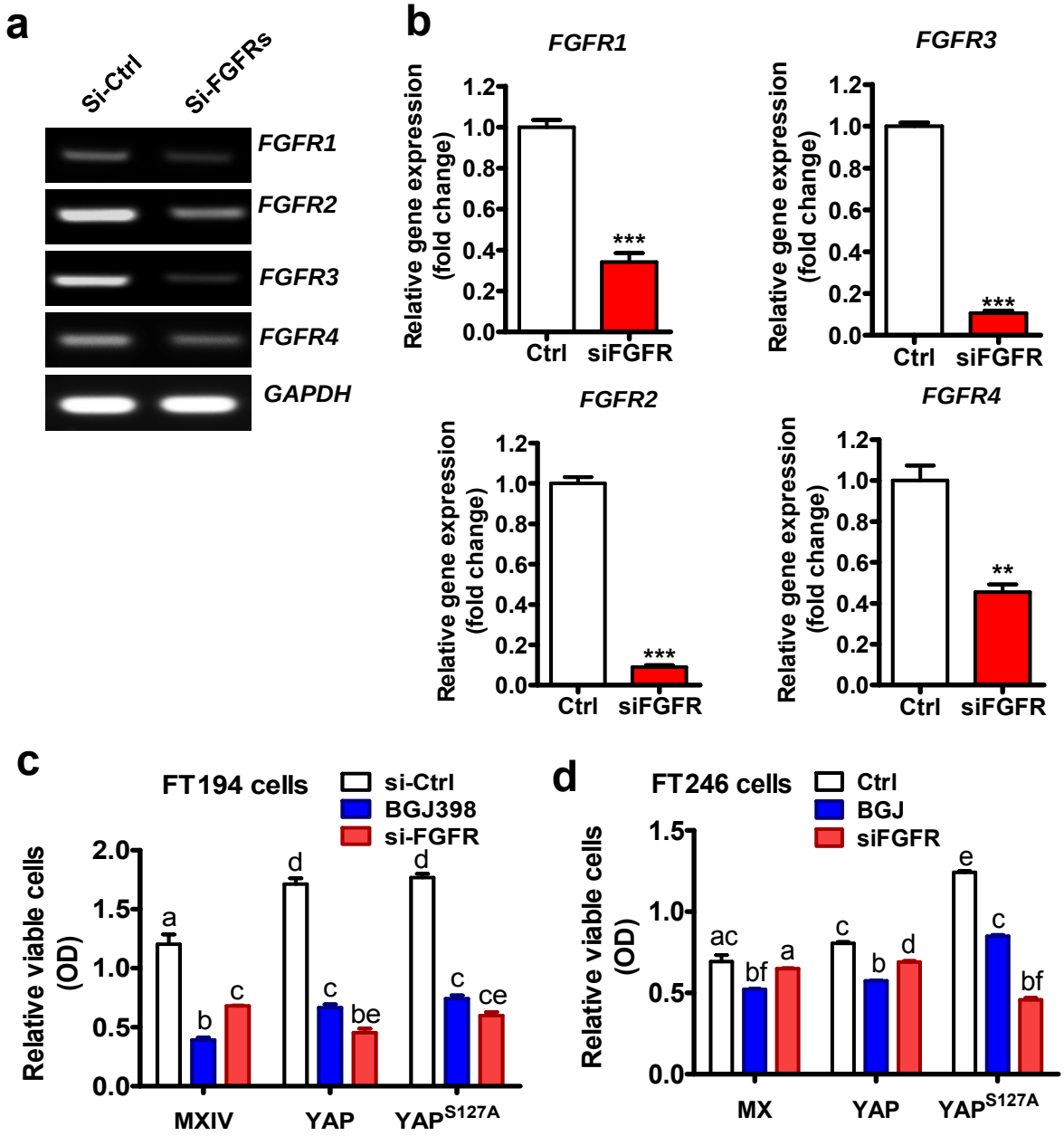


**Supplementary figure 22. Effect of FGFR knockdown on the growth of FTSECs.** FT194 and FT246 cells were transfected with non-targeting control siRNA (si-Ctrl) or siRNAs specifically target FGFRs (1-4). mRNA levels of FGFRs were determined by RT-PCR 72h after transfection. **a)** Representative images showing knockdown of FGFRs (1-4) with FGFR siRNAs in FT194 cells. **b**) quantitative data indicate the reduced FGFR (1-4) mRNA levels 72h after knockdown. **c & d**) MTT assay showing that knockdown of FGFRs in FT194 and FT246 cells abolished YAP- or constitutively active YAP-induced growth of FTSECs. BGJ was used as a positive control. Each bar represents the mean ± SEM of three independent assays. Bars with the same letter are not significantly different from each other.

Supplementary information

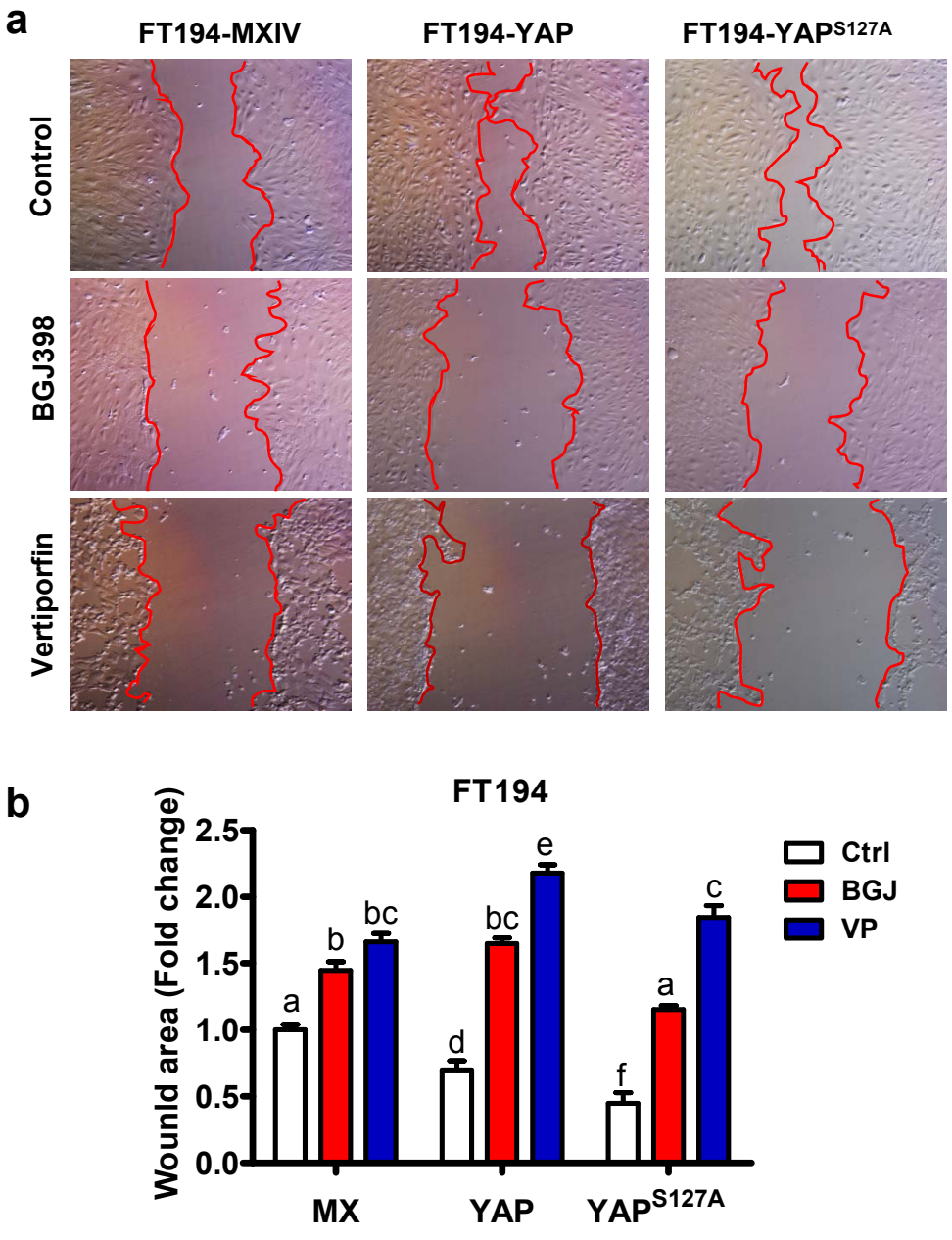


**Supplementary figure 23. Pharmacological inhibition of FGFRs or YAP activity blocked YAP-induced FTSEC cell migration. a**) Representative images showing the migration of FT194-MXIV (control), FT194-YAP and FT194-YAP$^{S127A}$ cells incubated in serum free medium for 15h. **b**) Quantitative data showing "wound" area fold changes in three FT194 cell lines (normalized to FT194-MXIV control group). Each bar represents the mean ± SEM of three independent assays. Bars with the same letters are not statistically different from each other ($P > 0.05$).

Supplementary information

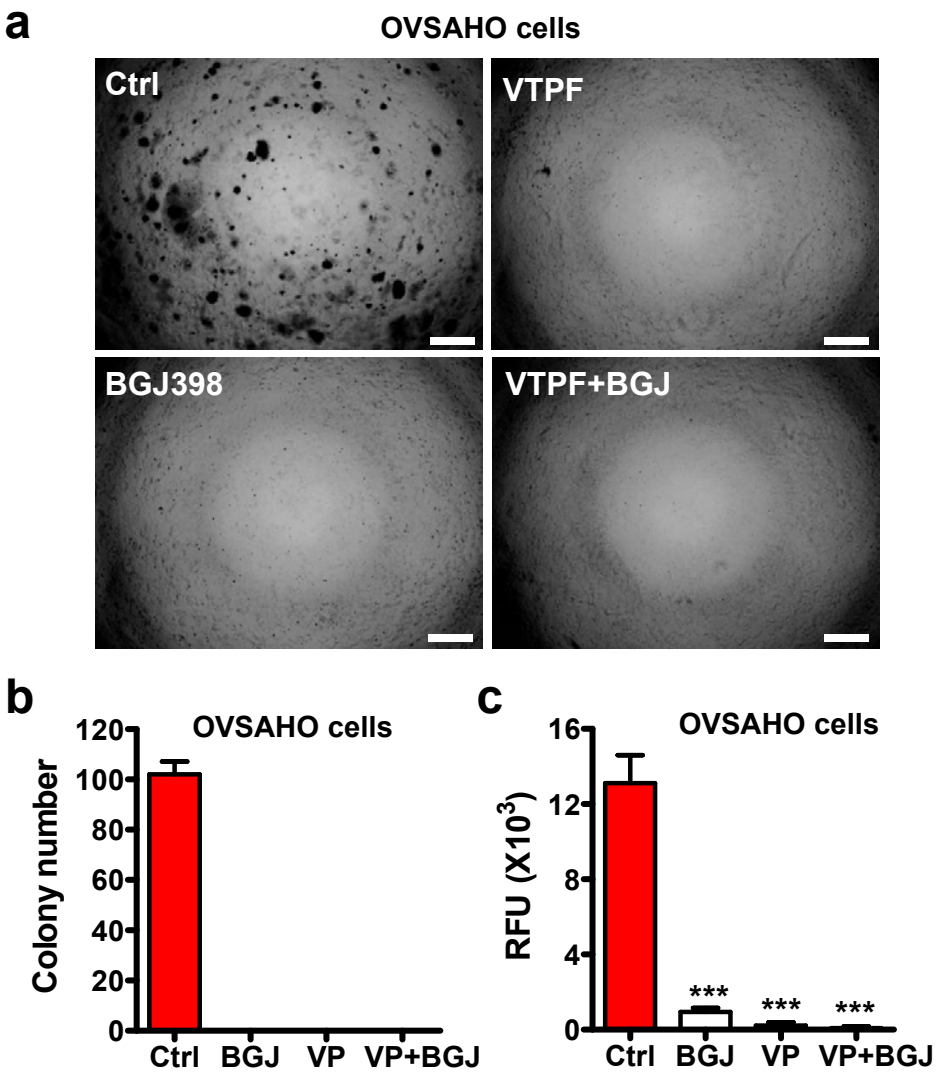


**Supplementary figure 24. Pharmacological blockage of FGFRs and YAP activity suppressed the growth of OVSAHO cells in the soft agar assay.** OVSAHO is a verified ovarian high grade serous carcinoma cell line (ref. 43). OVSAHO cells were incubated in a soft agar anchorage-free culture system with or without addition of BGJ398 (1μM) or vertiporfin (5μM). **a**) Representative images showing that verteporfin or/and BGJ398 abolished the colony formation ability of OVSAHO cells. **b**) Quantitative data showing colony number of OVSAHO cells with or without drug treatments. Each bar represents the mean ± SEM of three independent assays. **c**) Fluorescence-based quantitative soft agar assay showing that verteporfin or/and BGJ398 abolished the colony formation ability of OVSAHO cells. ***: $P < 0.001$ compared to control (0.1% DMSO). Scale bar: 500μm.

Supplementary information

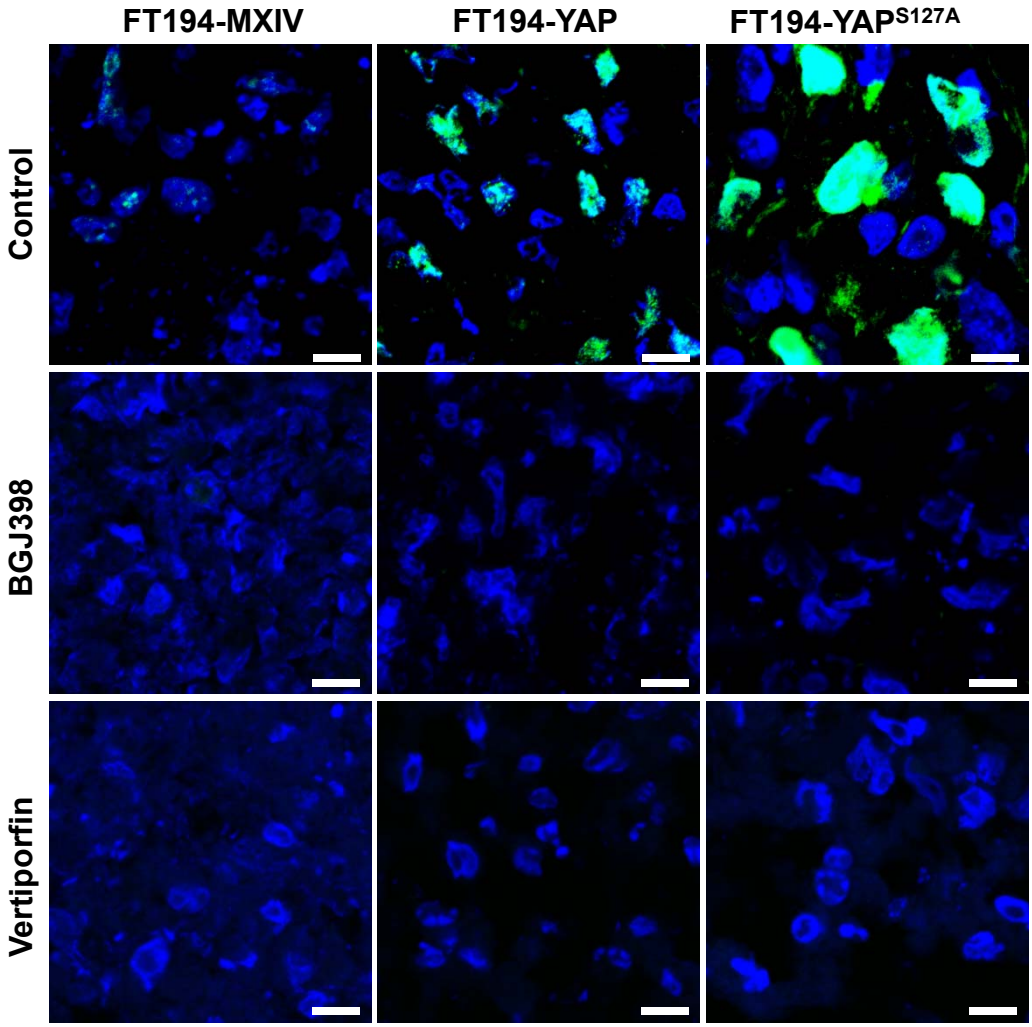


**Supplementary figure 25. Pharmacological blockage of FGFRs and YAP activity suppressed FTSEC cell death in a 3D hanging drop culture system**. FT194-MXIV, FT194-YAP and FT-194-YAP$^{S127A}$ cells were loaded onto a hanging drop culture system to form spheroids. The formed spheroids were then treated with or without BGJ398 (1μM) or vertiporfin (5μM) for 3 days before staining Ki-67 using fluorescent immunohistochemistry. Ki-67 positive cells are stained in green. Nuclei were stained with DAPI (blue). Scale bar: 10μm.

Supplementary information

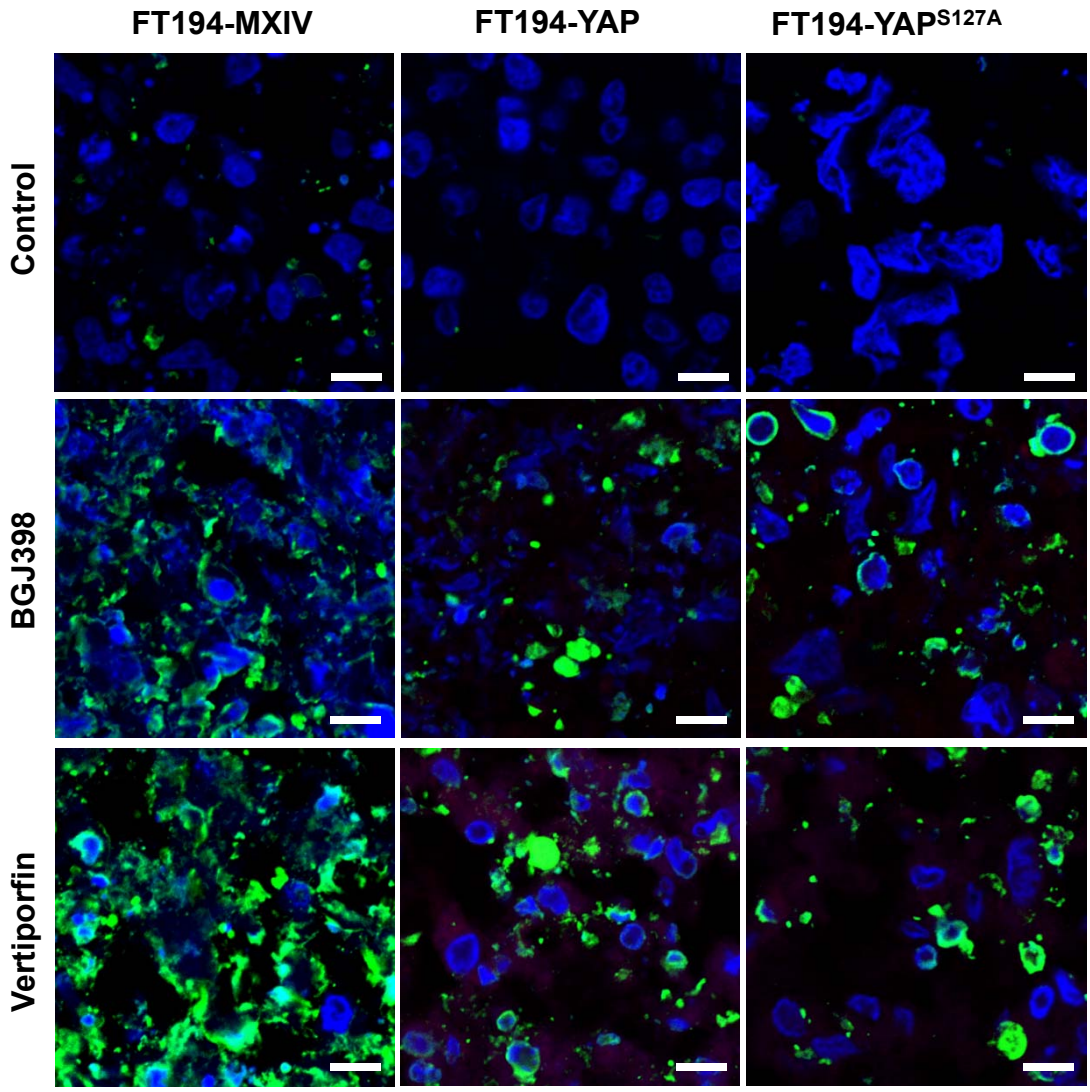


**Supplementary figure 26. Pharmacological blockage of FGFRs and YAP activity induced FTSEC cell death in 3D hanging drop culture system.** FT194-MXIV, FT194-YAP and FT-194-YAP$^{S127A}$ cells were loaded onto a 3D hanging-drop culture system to form spheroids. The formed spheroids were then treated with or without BGJ398 (1μM) or vertiporfin (5μM) for 3 days before TUNEL staining. The TUNEL positive cells (apoptotic cells) are stained in green. Nuclei were stained with DAPI (blue). Scale bar: 10μm.

Supplementary information

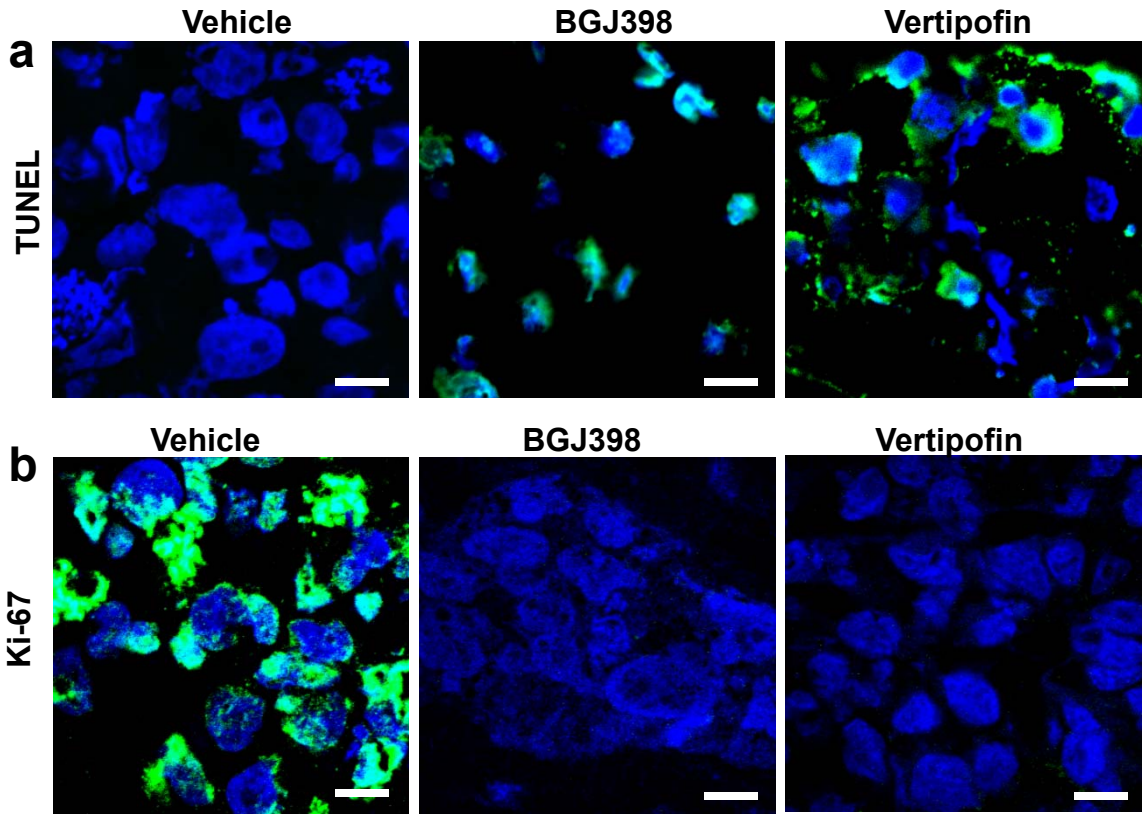


**Supplementary figure 27. Pharmacological blockage of FGFRs and YAP suppressed tumor cell proliferation and induced tumor cell death in incubated tumor xenografts derived from OVSAHO cells.** Tumor tissue slices derived from OVSAHO cell mouse xenografts were incubated with or without BGJ398 and verteporfin for 3 days. **a**) representative images showing the apoptotic cells determined by TUNEL assay. TUNEL positive cells (apoptotic cells) are stained with green. **b**): Representative images showing the expression of Ki-67 (green) stained by fluorescent immunohistochemistry. Nuclei were stained with DAPI (blum). Scale bar: 10μm.